Breaking Wave Impact on a Slender Cylinder

Jan Wienke[1], Uwe Sparboom[2] and Hocine Oumeraci[3]

Abstract

Large scale experiments have been conducted in the LARGE WAVE CHANNEL of the Forschungszentrum Küste (Coastal Research Centre) in Hannover to investigate the loads acting on a slender circular cylinder attacked by a breaking wave. The wave kinematics, the impact and the cylinder's response were measured simultaneously. For the load measurement two independent methods were used. On the one side pressures were measured and on the other side forces were determined at the bearings. Analysing the data a theoretical description for the two-dimensional impact is confirmed and peak values for the three-dimensional impact are obtained. It is shown that the commonly used calculation method for the impact force fails because the duration of impact is overestimated.

Introduction

Wave forces on slender cylinders are usually calculated by the Morison equation as a sum of the drag and the inertia force F_D and F_M which are considered as quasistatic:

$$F = F_D + F_M = \frac{1}{2} \cdot \rho \cdot C_D \cdot D \cdot U \cdot |U| + \rho \cdot C_M \cdot \frac{\pi \cdot D^2}{4} \cdot \dot{U} \qquad (1)$$

Looking at breaking waves the Morison equation must fail since the so calculated forces vary in time with the wave period whereas the impact due to wave breaking is of short duration. This impact cannot be considered by modifying the coefficients C_D and C_M in the Morison equation or by simply including a correction factor. Instead, an additional force must be introduced, so that the total force is

[1] Dipl.-Phys., Researcher, FORSCHUNGSZENTRUM KÜSTE (FZK) / "Coastal Research Centre", Merkurstrasse 11, D-30419 Hannover, Germany; wienke@fzk.uni-hannover.de
[2] Dr.-Ing., Senior Researcher, FORSCHUNGSZENTRUM KÜSTE
[3] Prof. Dr.-Ing., Member of Board of Directors, FORSCHUNGSZENTRUM KÜSTE

obtained as a sum of the so called quasistatic force calculated by the Morison equation and the impact force F_I.

$$F = F_D + F_M + F_I \tag{2}$$

The quasistatic force has often been examined and the Morison equation is a highly recognized tool for the calculation of this force. However, the impact force has yet been investigated only in a few test. Therefore, the impact force is the main subject of the recent investigations.

For the calculation of the impact force on slender cylinders, usually the method of von Karman is used (von Karman, 1929). As shown in figure 1(a), the cylinder is approximated by a flat plate with a width equal to the width of the immersed part of the cylinder at each instant of the impact. The force on the plate can be calculated by considering the potential flow below the plate and integrating the pressures calculated by the Bernoulli equation. The velocity of water vertical to the cylinder axis is constant for each instant and equal to the wave celerity C for a breaking wave. Applying the method of von Karman for the whole time of the impact (i.e. until the radius of the cylinder is immersed), the calculated line force decreases linearly with time. The line force is plotted in figure 3(c) (dashed line) and is given in equation 3 where ρ means the density of water and C_s the slamming coefficient.

$$f_I = \rho \cdot R \cdot C^2 \cdot C_s \qquad \text{with} \qquad C_s = \pi \cdot \left(1 - \frac{C}{R} \cdot t\right) \tag{3}$$

Von Karman's method is related to a cylinder of infinite length, i.e. the same force is acting at every part of the cylinder, that is the two-dimensional line force. Applying the method for breaking wave impact the two-dimensional force must be integrated over the height of the impact area as shown in figure 1(b). It was proposed that this height should be equal to λ multiplied with the maximum elevation of the wave at breaking η_b (Goda et al., 1966 and Wiegel, 1982). The parameter λ, called

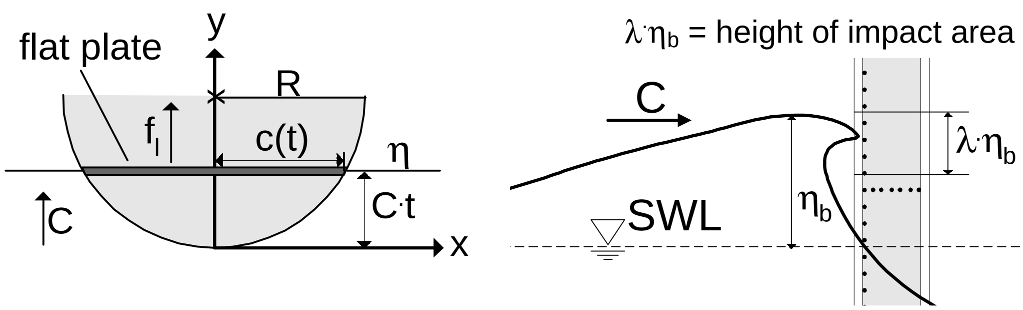

(a) Von Karman's model (b) Breaking wave impact

Figure 1. Application of von Karman's model to breaking wave impact on slender cylinders.

curling factor, depends on the breaker type.

$$F_I = \rho \cdot R \cdot C^2 \cdot C_s \cdot \lambda \cdot \eta_b \qquad (4)$$

Experimental set-up and procedure

The tests were carried out in the LARGE WAVE CHANNEL of the Forschungszentrum Küste in Hannover. This channel has an effective length of 309 m, a depth of 7 m and a width of 5 m. For the tests, the still water level was around 4 m. A sketch of the test set-up is given in figure 2. The test cylinder was installed on the flat bottom of the channel in a distance of 111 m from the wave paddle. Wave breaking was induced by superposition of several waves with different frequencies. So called Gaussian wave packets were used (Bergmann, 1985). These packets converge up to the point of concentration. At that location the wave packet becomes very steep and breaking must continue. The maximum elevation of the wave packets next to the point of concentration was around 2 m. For the tests the point of concentration was focussed in front of the cylinder and was varied over a certain distance.

The test cylinder is made of steel, has a length of 7.4 m and a diameter of 0.7 m. It is fixed at the bottom on the channel bed and at the top at a traverse structure. At the two bearings there are strain gauges installed to measure the total force in wave direction as the sum of the forces at the two bearings. Furthermore, 55 pressure transducers are installed in the cylinder. Some are installed in the front line and some others around the circumference of the cylinder.

15 wave gauges were installed in the wave channel to measure the elevation of the wave packets and to determine the wave celerity next to the point of

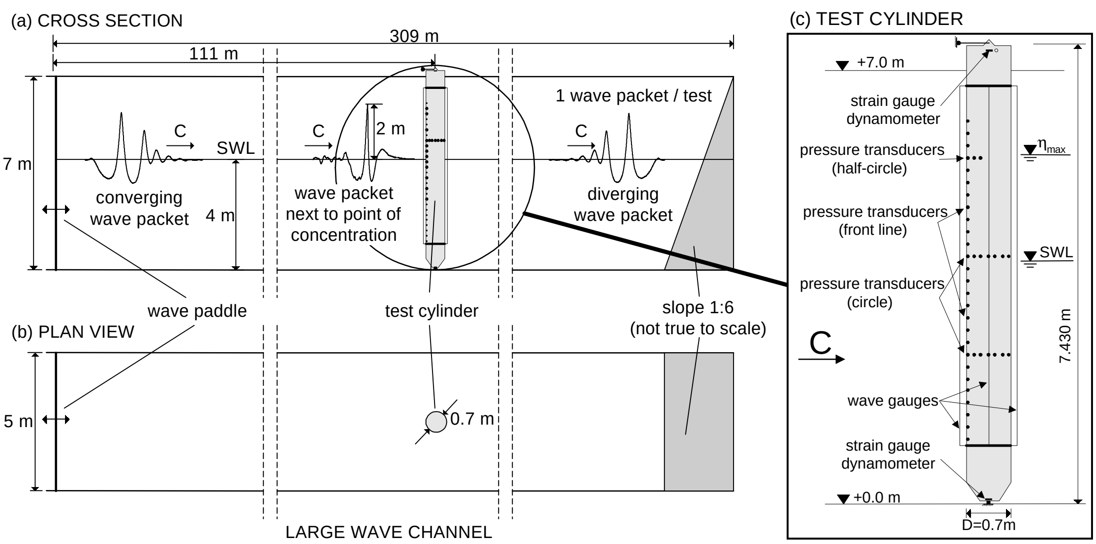

Figure 2. Experimental set-up and details of the test cylinder.

concentration. It was around 6 m/s. The water particle velocity was measured with 10 current meters at different levels. Comparing the measured maximum horizontal particle velocity of one test with the respective wave celerity, the equality of these two speeds was confirmed. So the dependence of the impact force on the square of the wave celerity is justified (see equation 3).

The generated wave packets are quite similar for each test. The celerity of the breaking wave is around 6 m/s, the maximum elevation varies between 1.6 m and 2 m, the steepness is around 0.1, only plunging breaking occurs. The main parameter being varied in the tests was the distance between the breaking location and the test cylinder. This variation is shown in the first four columns of table 1. With each row the varied distance is decreasing. The tests were subdivided up into 5 loading cases which are illustrated in table 1. Loading case 1 means that wave breaking occurs far in front of the test cylinder. Looking at loading case 2 it can be seen that the distance has decreased while for loading case 3 wave breaking occurs immediately in front of the cylinder. Wave breaking of loading case 4 takes place directly at the cylinder and waves of loading case 5 do not break in front of the cylinder but at the rear. The distinction between these cases was performed by the visual consideration of the tests and the transition between the cases is of course continual.

2-D impact: line force

Usually line forces are obtained by the integration of measured pressures, but in the area of impact this integration is not justified. The local and temporal distribution of the impact pressures is not resolved by interpolating the measured pressures for the integration. Therefore, the line forces must be determined theoretically and the related pressures can be compared to the experimentally determined values.

Comparing the pressures calculated with the theory of von Karman to the pressures measured with the pressure transducers at the half circle in the height of the wave crests (see figure 2(c)), no good agreement was found. The calculated pressures are much lower than the measured ones and the calculated instants of immersion take place significantly later than the measured. This is not really surprising since this disagreement is related to the so called pile-up effect which was theoretically predicted by Wagner (1932) but not considered in the von Karman model (figure 3). Concerning the breaking wave impact on a slender cylinder, the differences between the theories of von Karman and Wagner have already been reported by Tanimoto et al. (1986).

In the same way as von Karman did, Wagner approximated the circle by a flat plate and considered the potential flow around that plate. The force on the plate is calculated by considering the potential flow below the plate and integrating the pressures calculated by the Bernoulli equation. In contrast to von Karman, Wagner took the flow beside the plate into account. Integrating this flow over the time the

No.	Load case	Video records	Principle sketch	Force-time history	Force characteristics
1	• wave breaking far in front of the cylinder • overcurling breaker tongue hits cylinder far below wave crest level • broken wave		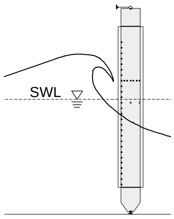	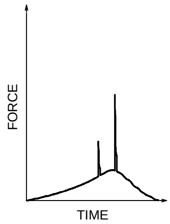	• double-peak • first peak is related to impact of breaker tongue • second peak due to impact of wave front • analysed as single peak, force will be overestimated by 20%
2	• wave breaking in front of the cylinder • breaker tongue hits cylinder just below wave crest level • splash upward and downward • breaking wave		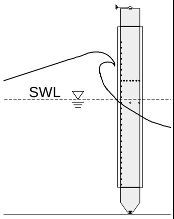	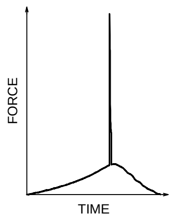	• single peak • highest impact force • due to assumption of simultaneous impact over the height, force might be overestimated by less than 20%
3	• wave breaking immediately in front of the cylinder • breaker tongue hits cylinder at wave crest level • radial splash • breaking wave		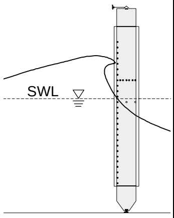	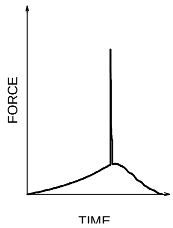	• single peak • assumption of simultaneous impact over the height is best fulfilled • highest accuracy for force evaluation is achieved for this case
4	• wave breaking at the cylinder • damped impact due to cylinder wave run-up • splash upward • partial breaking wave		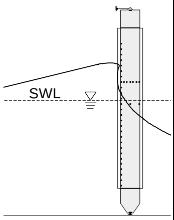	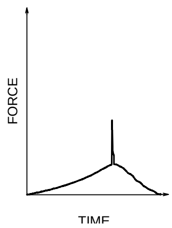	• single peak • duration of impact might be under-estimated due to cylinder wave run-up damping the impact • force might there-fore be considerably overestimated
5	• no wave breaking in front of the cylinder • quasistatic force • breaking wave at rear of cylinder		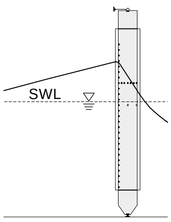	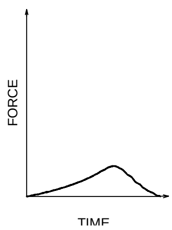	• no impact, only quasistatic force • total force obtained directly from the measurement at the bearings of the cylinder

Table 1. Classification of different loading cases.

pile-up effect is obtained as sketched in figure 3(b). Due to this effect the instant of immersion takes place earlier, the duration of impact decreases and the maximum line force increases. In figure 3(c) the time history of the calculated line forces is plotted. The line force calculated by the application of Wagner's theory is twice the line force calculated by von Karman's theory at the instant of first contact between water and cylinder.

That the description following the theory of Wagner is in good agreement to the measurements can be shown by the comparison of measured and calculated pressures at the half circle at the height of the wave crests (see figures 2(c)). In the 4 graphs of figure 4, the pressure histories are compared for seven different locations on the half circle. The pressure transducers are installed symmetrically to the front line A(0°) of the cylinder. So two pressure time histories at a time are expected to be equal. The solid line is the calculated pressure time history and the dashed lines are the measured ones. A fairly good agreement is found in this example. Only in graph A there is a considerable deviation. This is a typical effect in the front line (location of first contact between water and cylinder) which is caused by air inclusion. Water compressibility cannot be observed since this effect is of such a short duration that it is not resolved by the pressure measurement (Korobkin, 1996).

3-D impact: total force

The total force is determined independently of the pressure measurement by force measurement at the bearings of the test cylinder. So the problems associated with the pressure integration are avoided in this case. In figure 5 the measured total force time histories are shown. The graph A on the left represents a typical measured total force time history for a breaker of loading case 1 to 4 (see table 1). When the impact takes place the cylinder starts to oscillate. So at the bearings the acting force is not measured directly but also the response of the test cylinder is detected. The

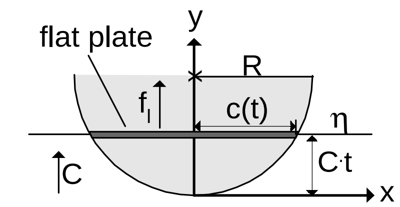

(a) Von Karman's model

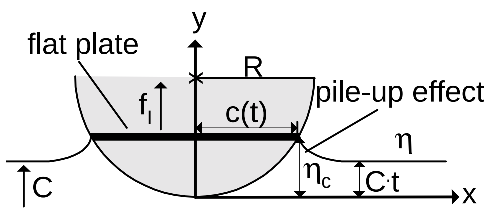

(b) Wagner‘s model

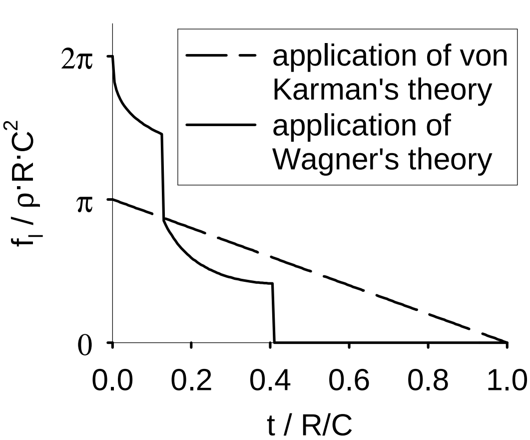

(c) Comparison of von Karman’s and Wagner‘s model

Figure 3. Horizontal section of the cylinder and calculated line force.

graph B in the middle contains a plot of the measured total force time history for a breaker of loading case 5. The wave packet is similar to the wave packet related to the left plot, but the breaking location is at the rear of the cylinder. So there is no impact force acting and no noticeable oscillation of the cylinder takes place. This force time history is equal to the quasistatic force time history. Calculating the difference of these two plots the oscillation shown in graph A-B on the right of figure 5 is obtained. This time history can be related to the impact force of the breaking wave, i.e. it represents the dynamic part of the force. For analysing this plot the acting force and the response part must be separated. This separation can be performed by deconvolution.

The deconvolution is the inversion of the convolution. Convolution is described by the following integral:

$$D(t)=\int_0^t E(x)\cdot i(t-x)dx=\tilde{E}(\omega)\cdot\tilde{i}(\omega) \qquad (5)$$

D is the directly recorded signal, i.e. the time history measured with the strain gauges at the two bearings of the test cylinder. *E* means the excitation function, i.e. the time history of the unknown actual acting force. The function *i* is the response of the detector which represents the damped oscillation of the test cylinder. The frequency and the damping coefficient of this oscillation are determined in preliminary tests. $\tilde{E}$ and $\tilde{i}$ are the Fourier transform functions. The convolution theorem states that the convolution integral is equal to the product of the Fourier

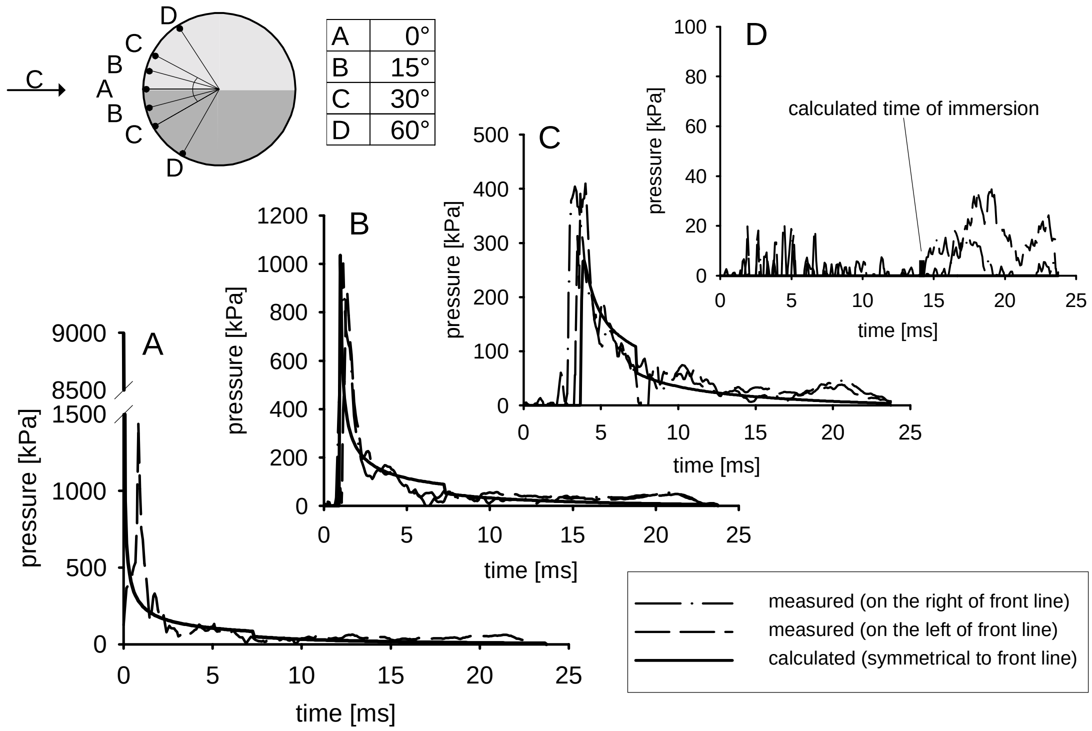

Figure 4. Impact pressure time histories at different locations.

transform functions. So the inversion of the convolution corresponds to a division by a Fourier transform function. Since this function is not different from zero for the whole domain of definition, it is obvious that the inverse function is not defined.

So the deconvolution is solved numerically to determine the actual acting wave force *E*. A basic approach for the unknown function *E* is used. The convolution of the approach with the cylinder's response *i* is calculated and the result is compared with the directly recorded signals *D*. To fit the calculated and the measured time histories the approach is multiplied with a factor. The value of this factor is determined by minimizing the deviation between the two time histories.

The functional dependence of the approach on time is not varied. It is assumed that the time history of the total force is equal to the time history of the line force shown in figure 3(c) (solid plot). This means that the force is acting at the same time over the whole height of impact. The same assumption is used for the transition from equation 3 to equation 4. The accuracy of this assumption is dependent on the loading case. For loading case 3 it is best fulfilled, while for the other loading cases the inaccuracy of the assumption must be considered as given in the last column of table 1. Originally, the assumption of simultaneous impact is related to a vertical breaker front. Considering the area of impact it can be shown theoretically that the assumption is justified when the angle between breaker front and cylinder axis is small. The pressure time histories measured in the front line of the cylinder are in agreement with the assumption of simultaneous impact. The delay of maximum

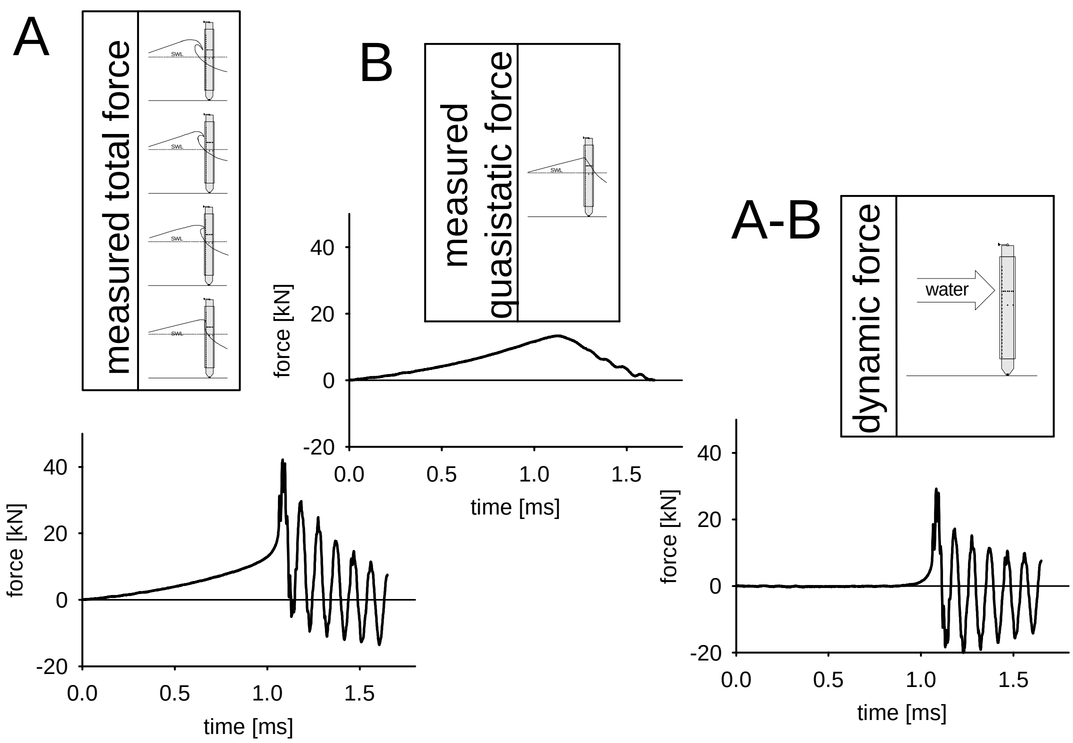

Figure 5. Total force time history and separation into dynamic and quasistatic part.

pressure along the front line in the area of impact is less than 20% of the duration of impact.

An illustrative example for the determination of the actual acting force is given in figure 6. In figure 6(a) the measured dynamic part of the force which is the thin solid line is deconvoluted by fitting the approach (thick line) so that the difference between the thin dashed and the thin solid lines is minimum. The dashed line is the convolution of the approach with the cylinder's response. After the impact force component has been determined in this way, the quasistatic force is added. The convolution for the summed up force is calculated and compared to the measured total force as shown in figure 6(b). The calculation procedure is completed when a good agreement between calculated and measured time histories is achieved.

The method for the analysis of the measured total forces is summed up in figure 7. On the left side there are the measured forces – the total force related to a breaking wave and the quasistatic force. Through the difference of these two forces, the dynamic force is obtained and then deconvoluted by using the theoretical approach following the theory of Wagner. In this way the impact force is obtained and added to the quasistatic force so that the total force acting on the cylinder would result. For verification, this total force is convoluted with the cylinder's response and compared to the measured total force.

Selected Results

A general overview of the results is given for all loading cases in the fifth column of table 1. For loading case 1 typically a double peak is obtained for the impact, for loading cases 2 to 4 only single peaks with a decreasing intensity are yielded. Since the accuracy of the method is highest for loading case 3 the difference in impact intensity between loading case 2 and 3 is not significant, but the intensity of impact for loading case 4 is obviously smaller.

In figure 8 the experimentally determined values are shown. At the top the

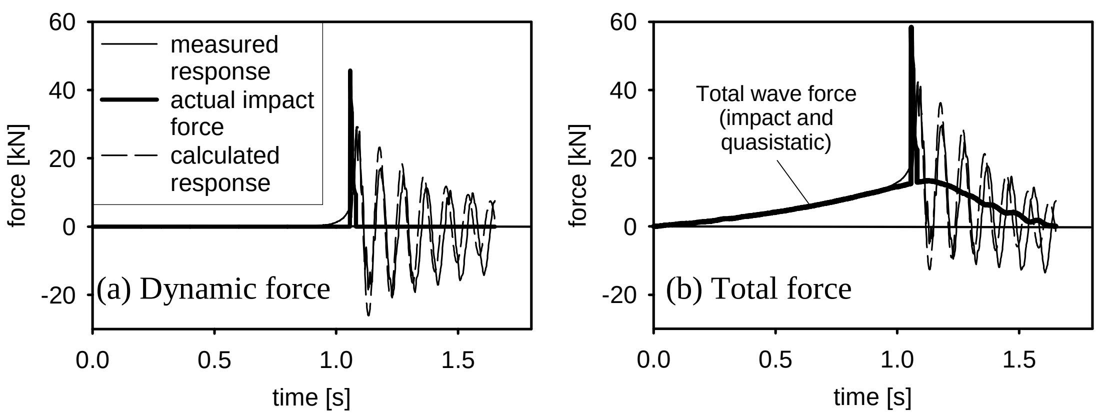

Figure 6. Dynamic part of the force (a) and total force (b).

maximum total force is plotted for the different loading cases. The highest values, up to almost 100 kN, are obtained for loading case 2. For loading case 3 values of more than 80 kN are determined. The quasistatic force which is related to loading case 5 is between 10 kN and 20 kN.

The graph below, quite similar, shows the impact force, i.e. the total force shown above without the quasistatic part of the force. Of course for loading case 5 there is no impact force, so the value is zero. The maximum values related to loading cases 2 and 3 are around 80 kN.

In the graph at the bottom the curling factor λ is plotted for the different loading cases (see introduction and figure 1(b)). The height of the impact area on the cylinder is given as λ multiplied with the maximum elevation (figure 1(b)). λ is the quotient of the impact force shown in the middle graph and the impact line force divided by the maximum elevation of the breaking wave. The maximum values for the curling factor are in good agreement with the values for plunging breakers given in literature (e.g. Goda et al., 1966 and Wiegel, 1982).

The curling factor is not only dependent on the type of breaker, but also on the distance between breaking location and cylinder. Only for loading cases 2 and 3, λ is maximum. For the other cases, the curling factor is lower. In these cases, the impact is damped for example by the cylinder wave run-up (loading case 4). If the impact does not take place at the same time over the height of impact (loading case 1) the maximum value of the force is also reduced, as well as the curling factor.

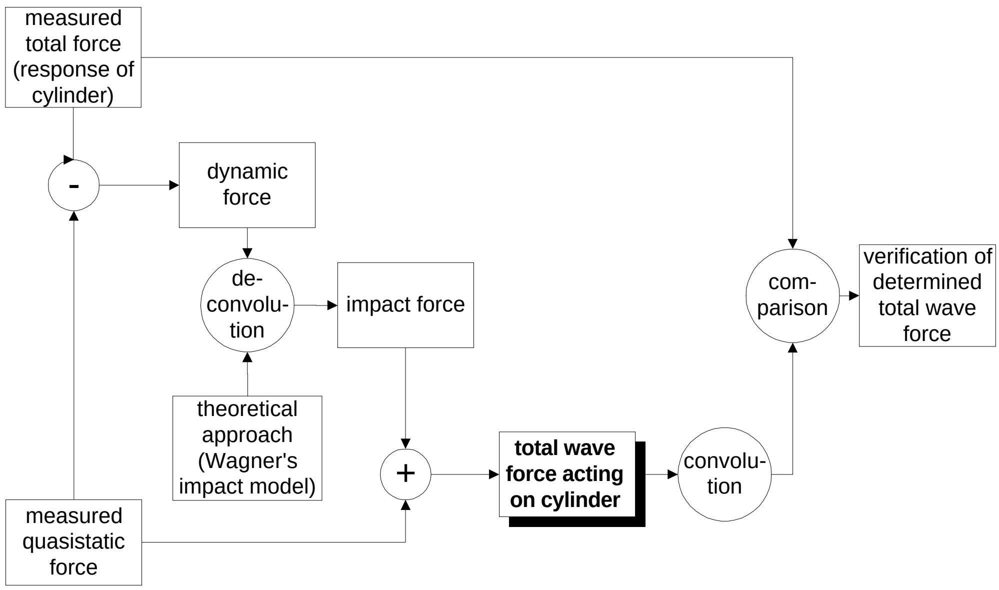

Figure 7. Diagram of the method for the analysis of the measured forces.

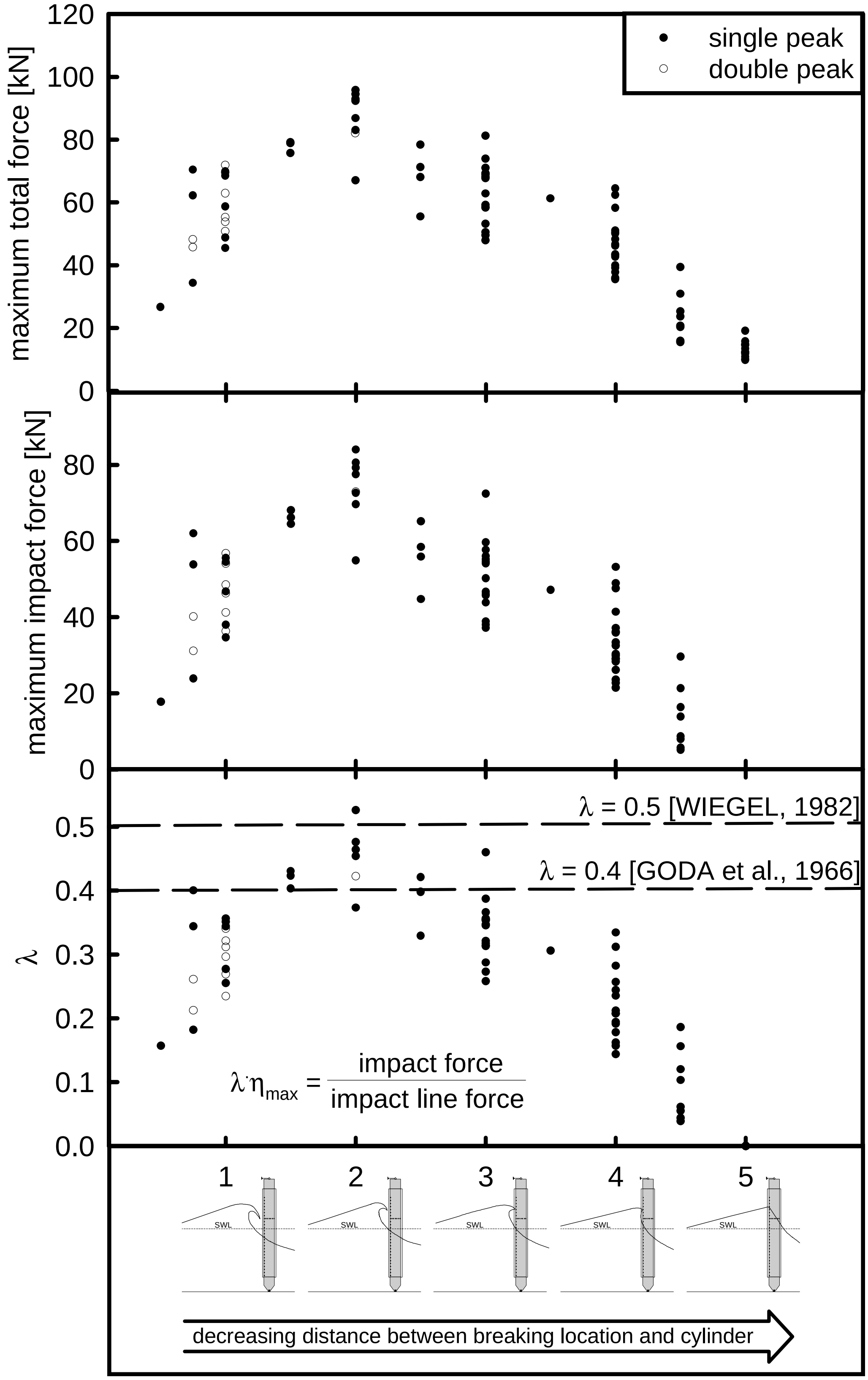

Figure 8. Experimentally determined values for the different loading cases.

Concluding Remarks

A theoretical two-dimensional description of the breaking wave impact force on a slender cylinder has been experimentally confirmed. The maximum value for this line force is twice the value commonly used. Furthermore, it is shown that the factor which is used to transform the two-dimensional description to a three dimensional one - the curling factor λ - is in agreement with the values given in literature.

So it is concluded that the commonly used method for the calculation of breaking wave impact fails for the breaking waves used in the presented experiments. The maximum values are twice the values calculated with the commonly used method. The pile-up effect influences both, the intensity and duration of impact and must be taken into consideration.

References

Bergmann, J. (1985). "Gaußsche Wellenpakete – Ein Verfahren zur Analyse des Seegangsverhaltens meerestechnischer Konstruktionen." *Thesis*, Technical University of Berlin (in German).

Goda, Y., Haranaka, S. and Masahat, M. (1966). "Study on impulsive breaking wave forces on piles." *Report*, Port and Harbour Technical Research Institute, 5, 6, 1-30 (in Japanese) reported in: Sawaragi, T. and Nochino, M. (1984). "Impact forces of nearly breaking waves on a vertical circular cylinder." *Coastal Engineering in Japan*, 27, 249-263.

Von Karman, T. (1929). "The impact on seaplane floats during landing." *Technical Note No. 321*. National Advisory Committee for Aeronautics.

Korobkin, A.A. (1996). "Water impact problems in ship hydrodynamics." *Advances in Marine Hydrodynamics*, Computational Mechanics Publications.

Tanimoto, K., Takahashi, S., Kaneko, T. and Shiota, K. (1986). "Impulsive breaking wave forces on an inclined pile exerted by random waves." *Proceedings of the 20th International Conference on Coastal Engineeering*, ASCE, 2288-2302.

Wagner, H. (1932). "Über Stoß- und Gleitvorgänge an der Oberfläche von Flüssigkeiten." *Zeitschrift für angewandte Mathematik und Mechanik*, 12, 4, 193-215 (in German).

Wiegel, R.L. (1982). "Forces induced by breakers on piles." *Proceedings of the 18th International Conference on Coastal Engineering*, ASCE, 1699-1715.